

This discussion paper is/has been under review for the journal Atmospheric Chemistry and Physics (ACP). Please refer to the corresponding final paper in ACP if available.

Analysis of the PKT correction for direct CO₂ flux measurements over the ocean

S. Landwehr¹, S. D. Miller², M. J. Smith³, E. S. Saltzman⁴, and B. Ward¹

¹School of Physics and Ryan Institute, National University of Ireland Galway, Galway, Ireland

²Atmospheric Sciences Research Center, University at Albany, State University of New York, Albany, New York, USA

³National Institute of Water and Atmospheric Research (NIWA), Private Bag 14-901 Kilbirnie, Wellington, New Zealand

⁴Department of Earth Sciences, University of California, Irvine, CA, USA

Received: 17 October 2013 – Accepted: 23 October 2013 – Published: 31 October 2013

Correspondence to: B. Ward (bward@nuigalway.ie)

Published by Copernicus Publications on behalf of the European Geosciences Union.

Title Page

Abstract

Introduction

Conclusions

References

Tables

Figures

◀

▶

◀

▶

Back

Close

Full Screen / Esc

Printer-friendly Version

Interactive Discussion



Abstract

Eddy covariance measurements of air–sea CO₂ fluxes can be affected by cross-sensitivities of the CO₂ measurement to water vapour, resulting in order-of-magnitude biases. Well established causes for these biases are (i) cross-sensitivity of the broad-band non-dispersive infrared sensors due to band-broadening and spectral overlap (commercial sensors typically correct for this) and (ii) the effect of air density fluctuations (removed by determining the CO₂ mixing ratio respective to dry air). However, another bias related to water vapour fluctuations has recently been observed with open-path sensors, and was attributed to sea salt build-up and water films on sensor optics. Two very different approaches have been used to deal with these water vapour-related biases. Miller et al. (2010) employed a membrane drier to physically eliminate 97% of the water vapour fluctuations in the sample air before it enters the gas analyser. Prytherch et al. (2010a), on the other hand, employed the empirical (Peter K. Taylor, PKT) post-processing correction to correct open-path sensor data. In this paper, we test these methods side by side using data from the Surface Ocean Aerosol Production (SOAP) experiment in the Southern Ocean. The air–sea CO₂ flux was directly measured with four closed-path analysers, two of which were positioned down-stream of a membrane dryer. The CO₂ fluxes from the two dried gas analysers matched each other and were in general agreement with common parametrisations. The flux estimates from the un-dried sensors agreed with the dried sensors only during periods with low latent heat flux ($\leq 7 \text{ W m}^{-2}$). When latent heat flux was higher, CO₂ flux estimates from the un-dried sensors exhibited large scatter and an order-of magnitude bias. We applied the PKT correction to the flux data from the un-dried analysers and found that it did not remove the bias when compared to the data from the dried gas analyser. Our detailed analysis of the correction algorithm reveals that this method is not valid for the correction of CO₂ fluxes.

Analysis of the PKT correction

S. Landwehr et al.

Title Page

Abstract

Introduction

Conclusions

References

Tables

Figures

◀

▶

◀

▶

Back

Close

Full Screen / Esc

Printer-friendly Version

Interactive Discussion



1 Introduction

Direct measurements of air–sea CO₂ flux contribute to the understanding of the Earth climate system and can be used to study the fundamental physics of air–sea gas exchange. When direct flux measurements are combined with the measurement of the partial pressure gradient of CO₂ across the air–water interface, $\Delta p\text{CO}_2$, the gas transfer velocity k can be derived as follows (e.g. Wanninkhof, 1992):

$$k = \frac{F_c}{S \cdot \Delta p\text{CO}_2} \quad (1)$$

where S is the solubility of CO₂ in sea water and F_c is the vertical CO₂ flux. The ability to parametrise k is essential for modelling global air–sea CO₂ fluxes based on $\Delta p\text{CO}_2$ climatologies (Takahashi et al., 2002), and for increasing our understanding of the global oceanic uptake of CO₂ (Ward et al., 2004).

In the eddy covariance (EC) method, the turbulent flux is directly calculated from the covariance of the fluctuations in the vertical wind speed (w') and fluctuations in the CO₂ mixing ratio in dry air (x'_c):

$$F_c = \langle n_d \rangle \langle w' x'_c \rangle \quad (2)$$

where n_d is the dry air density (here $\langle \rangle$ indicates a time average over a time interval t_i and the primes denote deviations from the mean). The w' and x'_c parameters need to be sampled fast enough to resolve the smallest flux-carrying eddies (typically 10 Hz), and the averaging interval needs to be long enough to include large scale motions that contribute to the vertical flux, but short enough to ensure stationarity of the relevant parameters during the interval (typically t_i are between 15–60 min) (Kaimal et al., 1972). The EC method thus allows the study of gas transfer with much higher time resolution than both dual tracer experiments (Nightingale et al., 2000; Ho et al., 2006) and measurements of the ¹⁴C concentration in sea water (Wanninkhof, 1992).

Commonly-used broadband infrared gas analysers (IRGA), such as LICOR LI7500 and LI7200, measure the CO₂ concentration n_c (number of molecules per volume),

Title Page

Abstract

Introduction

Conclusions

References

Tables

Figures

◀

▶

◀

▶

Back

Close

Full Screen / Esc

Printer-friendly Version

Interactive Discussion



Analysis of the PKT correction

S. Landwehr et al.

Title Page

Abstract

Introduction

Conclusions

References

Tables

Figures

◀

▶

◀

▶

Back

Close

Full Screen / Esc

Printer-friendly Version

Interactive Discussion



from which the mixing ratio needs to be calculated. Therefore, simultaneous measurements of temperature T , pressure P , and water vapour concentration n_v are necessary to calculate the dry air density and the CO_2 mixing ratio $x_c = n_c n_d^{-1}$ (Webb et al., 1980). Equation (2) can be written as the sum of the flux measured by the IRGA and a bias flux, caused by the fluctuations of the dry air density $n_d = (P/RT - n_v)$, i.e.:

$$F_c = \underbrace{\langle n'_c w' \rangle}_{\text{IRGA}} + \underbrace{\langle x_c \rangle \cdot \left[\langle n'_v w' \rangle + \frac{\langle n_d + n_v \rangle}{\langle n_d \rangle} \cdot \left(\frac{\langle T' w' \rangle}{\langle T \rangle} - \frac{\langle P' w' \rangle}{\langle P \rangle} \right) \right]}_{\text{air density fluctuations}} \quad (3)$$

For CO_2 , the bias terms can easily exceed the vertical flux by an order of magnitude because the fluctuations x'_c are small compared to the background $\langle x_c \rangle$ (Webb et al., 1980). Equations (3) and (2) are fully equivalent.

EC is considered a standard method over land, but the application over the open ocean has proved to be more challenging. In the case of ship-based studies, the wind speed measurement needs to be carefully corrected for platform motion (e.g. Edson et al., 1998; Miller et al., 2008). Over land, the pressure term in Eq. (3) can be ignored, but at sea the platform motion-induced pressure fluctuations can introduce a further bias flux as they may correlate with residuals of ship motion signal in the motion-corrected wind speed (Miller et al., 2010). CO_2 fluxes over the ocean are typically much smaller than over land, and with currently available sensor technology, the EC method is restricted to areas with high air–sea gradients $\Delta p\text{CO}_2 \geq 40 \mu\text{atm}$ (Rowe et al., 2011).

For EC, the trace gas measurement has to be carried out on the same air sample as the wind speed measurement. This can be done directly using an open-path (OP) IRGA, which is located close to the sonic anemometer (Kondo and Osamu, 2007; Yelland et al., 2009; Prytherch et al., 2010b). Alternatively, air can be pumped to a distant closed-path (CP) IRGA, at a sufficiently high flow rate (e.g. McGillis et al., 2001). This allows deliberate pre-conditioning of the air sample, such as removal of the temperature and water vapour fluctuations and the application of in-line particle filters to avoid

Analysis of the PKT correction

S. Landwehr et al.

Title Page

Abstract

Introduction

Conclusions

References

Tables

Figures

◀

▶

◀

▶

Back

Close

Full Screen / Esc

Printer-friendly Version

Interactive Discussion



the deposition of salt or dust particles on the sensor lenses. McGillis et al. (2001) were the first to carry out EC measurements of the air–sea CO_2 flux, which were in general agreement with common bulk flux formulae. Miller et al. (2010) developed a CP system, where 97 % of the water vapour flux signal is removed by passing the air flow through a membrane dryer. This significantly lowered the magnitude of the air density correction term in Eq. (3).

Attenuation of the fluctuations within the sample tube of CP systems can lead to an underestimation of the turbulent transport carried by the small high frequency eddies (Leuning and King, 1992). To minimise this effect, a high flow rate ($\mathcal{O}(100)$ slpm) must be maintained. Therefore, CP systems have higher power and maintenance requirements than OP systems.

In the oceanic environment, the lenses of OP IRGAs are prone to the build-up of salt particles, and flushing with fresh water is necessary to avoid degradation of the signal. The LI7500 has also been deployed with a shroud and a very high airflow (570 slpm) (Edson et al., 2011). This deployment mode is a hybrid of the OP and CP mode as the contamination with sea spray is reduced with minimal loss of high frequency fluctuations. Even when the air density correction Eq. (3) has been applied carefully, reported CO_2 flux values based on OP and shrouded OP EC systems over the open ocean are typically an order of magnitude higher than expected based on generally accepted bulk flux parametrisations (Kondo and Osamu, 2007; Prytherch et al., 2010a; Lauvset et al., 2011; Edson et al., 2011).

The exact reason for the additional bias is still unclear. Kohsiek (2000) suggested that the build-up of water films on the sensor lenses could lead to a biased CO_2 measurement x_{cm} with dependency on the relative humidity (RH). This will cause a bias in the CO_2 flux measurement F_{cm} , which scales with the latent heat flux because the fluctuations of the water vapour concentration in the sample volume will lead to artificial fluctuations in x_{cm} . Removing this artificial cross-correlation is difficult because there is a natural correlation between the fluctuations of the two scalars x_c and x_v , which are both transported by the same turbulent eddies. Attempting to remove the artificial

Analysis of the PKT correction

S. Landwehr et al.

Title Page

Abstract

Introduction

Conclusions

References

Tables

Figures

◀

▶

◀

▶

Back

Close

Full Screen / Esc

Printer-friendly Version

Interactive Discussion



dependency $x_{cm}(RH)$ with regressions or polynomial fits can thus lead also to the removal of the turbulence-driven variations of x_c and, therefore, of the CO_2 flux signal itself. Prytherch et al. (2010a) suggested that the accumulation of salt particles on the lens of the LI7500 OP IRGA could modulate the magnitude of the bias. Edson et al. (2011) reported that the accumulation of salt particles on their shrouded and regularly cleaned IRGAs was unlikely and suggested that a more suitable explanation was provided by the contamination of the optics with small particles from the ship's engines combined with organic deposits from sea spray. Prytherch et al. (2010a) went further and presented a correction method (called the Peter K. Taylor – PKT – method), which has since been used in several publications to correct OP CO_2 fluxes (e.g. Prytherch et al., 2010b; Lauvset et al., 2011; Edson et al., 2011). A selection of the publications mentioned above are also listed in Table 1 together with a brief description of the deployed IRGAs and findings relevant to this contribution.

Here we show that even EC measurements using CP IRGAs can be affected by a large humidity bias when the sampled air is neither dried nor filtered. Even though the PKT method was originally designed for the correction of humidity flux-related biases in OP measurements, it does not include any OP-specific assumptions, nor a specification of the physical cause of the bias. Thus the application to un-dried CP data is a valid test of the method's ability to remove the observed humidity flux-related bias in broadband non-dispersive infrared (NDIR) sensors.

In the subsequent sections of this article we describe the EC flux systems that were deployed in the Surface Ocean Aerosol Production (SOAP) experiment and present the CO_2 flux results from the dried and un-dried CP systems with and without application of the PKT correction. We further analyse and discuss this correction method (Prytherch et al., 2010a) in detail.

2 Experiment and methods

The SOAP field campaign was conducted from February to March 2012 on the R/*Tangaroa*. The EC system described here consisted of two Csat3 sonic anemometers attached to the bow mast (12.6 m a.s.l.), which provide high frequency measurements of the three components of the wind vector (u , v and w) and the speed of sound temperature (T_s), as well as four IRGAs of the type LI7200 ($\times 2$) and LI7500 ($\times 2$), which were located inside the container laboratory on the bow deck and connected to the sample volume on the mast with a stainless steel tube (ID = 1 cm; $L = 20$ m). The inlet tube was heated to avoid condensation on the walls, which would lead to an underestimation of the EC latent heat flux. A pump (Gast model 1423) delivered a continuous air stream from the mast at 100 slpm. Figure 1 shows a schematic of the flux system.

A part of the main flow (17 slpm) was directed to the two LI7200s CP IRGAs (IRGA_{wet}) connected in sequence. Up to this point the air was not filtered. The air stream was subsequently divided and passed to two LI7500s, converted to CP (IRGA_{dry}), which were connected in parallel, each positioned downstream of a Nafion membrane dryer (PD-200T) to remove the water vapour fluctuations as shown by Miller et al. (2010). Zero air was injected periodically (every 6 h) into the sample inlet to measure the delay of the signal in the IRGAs. Pressure and temperature in each IRGA sample volume were also measured with external sensors (Mensor CPT6100 and a thermocouple, respectively). An inertial motion unit (IMU – Systron Donner MotionPak II) provided high frequency acceleration and rate data, and a GPS compass and the ship's gyrocompass were used to completely describe the ship's motion. These data allowed the wind speed measurements from the Csat3 to be corrected for platform motion following Miller et al. (2008). All measurements were performed at 10 Hz.

ACPD

13, 28279–28308, 2013

Analysis of the PKT correction

S. Landwehr et al.

Title Page

Abstract

Introduction

Conclusions

References

Tables

Figures

◀

▶

◀

▶

Back

Close

Full Screen / Esc

Printer-friendly Version

Interactive Discussion



2.1 Data analysis and flux calculations

The fluxes of momentum u_* and the sonic sensible heat H_{sonic} were calculated from the Csat3 data after motion correction (Miller et al., 2008) and rotation of the wind vector into the mean flow (McMillen, 1988). The latent heat flux HI was calculated from the covariance of the vertical wind speed w with the water vapour mixing ratio x_v from the IRGA_{wet} after correction for the time delay. H_{sonic} was corrected with the latent heat flux to derive the sensible heat flux H_s , following (Burns et al., 2012). The measured CO₂ density was converted into mixing ratio, and ship motion contaminations of the signal due to flexing of the sensor or inertial forces on the filter wheel were removed using a linear regression with the acceleration and rate signal (as in Miller et al., 2010).

All flux calculations were performed over 25 min intervals. These intervals were divided into five 5 min sub-intervals and were excluded if any of the mean wind direction within the sub-intervals exceeded $\pm 100^\circ$ to the bow to minimise flow distortion effects. Flux intervals were also excluded when spikes were present in the wind speed or IRGA measurements. The remaining intervals were checked for signs of non-stationarity in the CO₂ co-spectra of the two IRGA_{dry}, and the same criteria as in Bell et al. (2013) were applied. A total of 337 of 1039 intervals passed the quality control for the two IRGA_{dry} and were used for the analysis presented here. For IRGA_{wetA} and IRGA_{wetB}, only 273 and 263 intervals, respectively, passed because these analysers had been removed from the setup for about one day.

The PKT correction, as presented by Prytherch et al. (2010a), was applied to the mixing ratios measured by the two IRGA_{wet} analysers. This method includes an iteration in which the correct flux value is approximated. The termination criteria for the iteration was chosen according to Prytherch et al. (2010a), to be $|F_c^{(j)} - F_c^{(j-1)}| \leq 0.04 \text{ mol m}^{-2} \text{ yr}^{-1}$. Prytherch et al. (2010a) also suggested a rejection of the PKT results if the iteration did not converge within 10 steps or if $F_c^{(j)}$ exceeded $\pm 400 \text{ mol m}^{-2} \text{ yr}^{-1}$ (which was considered unrealistically high). Thus the application of the PKT correction to the IRGA_{wet} measurements lead to a further reduction of the data set. For IRGA_{wetA},

[Title Page](#)[Abstract](#)[Introduction](#)[Conclusions](#)[References](#)[Tables](#)[Figures](#)[◀](#)[▶](#)[◀](#)[▶](#)[Back](#)[Close](#)[Full Screen / Esc](#)[Printer-friendly Version](#)[Interactive Discussion](#)

the PKT correction rejected 99 of the 273 intervals and for IRGA_{wetB} 85 of 263, respectively. The fluxes calculated from measured x_{cm} and the PKT-corrected x_{PKT} were evaluated against the unbiased measurements of the IRGA_{dry}. These results are presented in Sects. 3.1 and 3.2, respectively.

The flux measurements are affected by air-flow distortion, which results in a bias that depends mostly on the relative wind direction (Popinet et al., 2004; O'Sullivan et al., 2013). For this submission, the measurements were not corrected for air flow distortion because we concentrate on the comparison of different IRGA signals that were all correlated with the same wind speed measurement. Air flow distortion does therefore not affect our conclusions.

3 Results

Figure 2 shows an overview of the conditions encountered during the SOAP experiment from 16 February–5 March 2012 (doy 47–65). The wind speed range was between 0–15 m s^{-1} (25 min average) and peaked at 20 m s^{-1} on doyp 61. Unfortunately, the uninterruptible power supply of the EC system was flooded during this storm event, leading to a 12 h gap in the record. The ship was steered into the wind as much as possible, except during survey periods or deployments of instruments. The air temperature was mostly colder than the water temperature (measured by the ship's thermosalinograph) except for a period between doyp 51 and 55, when a warm air mass led to negative turbulent heat fluxes. The air-water $p\text{CO}_2$ difference ranged between -40 and -120 μatm . These large $\Delta p\text{CO}_2$ values were easily within the 40 μatm criterion for EC flux measurements with the LICOR IRGAs (Rowe et al., 2011).

3.1 Primary CO₂ flux results

The CO₂ flux measurements from the four CP IRGAs (without PKT correction) are plotted in Fig. 3 (top and middle). The CO₂ flux estimates from the dry gas analysers were

Title Page

Abstract

Introduction

Conclusions

References

Tables

Figures

◀

▶

◀

▶

Back

Close

Full Screen / Esc

Printer-friendly Version

Interactive Discussion



in general agreement with each other and the widely-used parametrisation from Waninkhof (1992), while the flux measurements from the un-dried gas analyser exhibited large scatter.

The difference in the CO_2 flux measurements from the IRGA_{wet} and IRGA_{dry} , i.e. ($\text{IRGA}_{\text{wet}} - \text{IRGA}_{\text{dry}}$) is plotted in Fig. 4. The variance of the IRGA_{wet} flux data increased proportionally with the latent heat flux and became an order of magnitude larger than that from the IRGA_{dry} . The range of the bias was much larger for $\text{IRGA}_{\text{wetA}}$ than for $\text{IRGA}_{\text{wetB}}$.

However, the primary flux estimates from the two IRGA_{wet} sensors agreed with the IRGA_{dry} estimates during periods with very low latent heat flux ($\text{HI} \leq 7 \text{ W m}^{-2}$). These periods are marked as shaded areas in Fig. 3. The limit of 7 W m^{-2} was chosen so that the envelope of the bias was approximately two times the scatter observed at $\text{HI} \approx 0 \text{ W m}^{-2}$. Figure 5 shows scatter plots of the IRGA_{wet} against $\text{IRGA}_{\text{dryB}}$ for ($\text{HI} \leq 7 \text{ W m}^{-2}$) and of $\text{IRGA}_{\text{dryA}}$ against $\text{IRGA}_{\text{dryB}}$ for the whole data set. A linear regression of the $\text{IRGA}_{\text{dryA}}$ vs. $\text{IRGA}_{\text{dryB}}$ for the full dataset gave a slope of (1.09 ± 0.01) with a $R^2 = 0.96$. For $\text{IRGA}_{\text{wetA}}$ and $\text{IRGA}_{\text{wetB}}$ regression was performed over the restricted data set ($\text{HI} \leq 7 \text{ W m}^{-2}$) and gave slopes of (0.88 ± 0.15) with $R^2 = 0.36$ and (0.93 ± 0.06) with $R^2 = 0.78$, respectively.

Figures 6 and 7 (left side) show scatter plots of the primary flux measurements of $\text{IRGA}_{\text{wetA}}$ and $\text{IRGA}_{\text{wetB}}$ against $\text{IRGA}_{\text{dryB}}$ for the full data set. The magnitude of the latent heat flux is used as colour code. Linear regression of the IRGA_{wet} vs. $\text{IRGA}_{\text{dryB}}$ gave slopes of (-0.04 ± 0.8) for $\text{IRGA}_{\text{wetA}}$ and $(+0.7 \pm 0.1)$ for $\text{IRGA}_{\text{wetB}}$, respectively, both with very low R^2 values. On average, the effect of the bias was to reduce the CO_2 flux, even changing the sign.

3.2 Application of the PKT Correction to IRGA_{wet} measurements

The PKT correction, as presented by (Prytherch et al., 2010a), was applied to the x_{cm} measured by the two IRGA_{wet} analysers and the results were evaluated against the

Title Page

Abstract

Introduction

Conclusions

References

Tables

Figures

◀

▶

◀

▶

Back

Close

Full Screen / Esc

Printer-friendly Version

Interactive Discussion



Analysis of the PKT correction

S. Landwehr et al.

Title Page

Abstract

Introduction

Conclusions

References

Tables

Figures

◀

▶

◀

▶

Back

Close

Full Screen / Esc

Printer-friendly Version

Interactive Discussion



unbiased measurements of the IRGA_{dry}. Figure 3 (bottom) shows the PKT-corrected fluxes (F_c^{PKT}) as well as the results from Eq. (7), which is derived in Sect. 4 and presents a simplified version of the PKT correction that also provides an output when the PKT correction does not converge. The results of Eq. (7) are not used in the evaluation of the PKT correction results, i.e. intervals that were rejected by the PKT correction are excluded from the analysis.

Scatter plots in Figs. 6 and 7 show the correlation between the IRGA_{wet} and the fluxes from IRGA_{dryB} before (left) and after the application of the PKT correction (right). For low latent heat flux, the PKT correction increases the scatter of the initially well-correlated measurements and also rejects a large part of the results. For IRGA_{wetA}, the PKT correction reduces the large range of scatter, but it does not improve the correlation with the IRGA_{dryB} fluxes. For IRGA_{wetB}, which shows a weaker bias, the PKT correction even reduces the correlation with the IRGA_{dryB} flux estimates from (0.7 ± 0.1) to (0.4 ± 0.2) .

The average raw flux estimates from the four CP IRGAs and with PKT correction for the two IRGA_{wet} are shown in Table 2. The average was taken over the complete data set and over three subsets, which were based on the magnitude and sign of the latent heat flux measured by the IRGA_{wet}. For the whole cruise, the PKT correction brought the flux measurements from IRGA_{wetA} and IRGA_{wetB} into closer agreement. The mean estimate of the IRGA_{wet} after PKT did, however, underestimate the flux ($\overline{F_c} = -6.73 \text{ mol m}^{-2} \text{ yr}^{-1}$) by 80%. For Subset 1, ($[-7 \text{ W m}^{-2} \leq \text{HI} \leq +7 \text{ W m}^{-2}]$) the bias in the IRGA_{wet} was negligible and the flux estimates of all four sensors agreed within 10%. Here PKT changed the IRGA_{wet} by less than 15%. For Subset 2 with moderately negative latent heat fluxes ($[-35 \text{ W m}^{-2} \leq \text{HI} \leq -7 \text{ W m}^{-2}]$), the PKT correction increased the bias in the IRGA_{wet} flux estimate from 18% to 62%. Subset 3 included the largest latent heat fluxes ($[+7 \text{ W m}^{-2} \leq \text{HI} \leq 340 \text{ W m}^{-2}]$); here, the PKT-corrected fluxes are only small fractions of the dried fluxes i.e. -2% and +11% for IRGA_{wetA} and IRGA_{wetB}, respectively. The average flux estimates of the two IRGA_{dry} agreed within

1% for the whole cruise and for subsets 1 and 3. For subset 2 the agreement was within 3%.

4 Analysis of the PKT correction

In the light of the unsatisfactory results of the PKT correction (cp. Sect. 3.2), we will now analyse the correction algorithm in detail.

The PKT method Prytherch et al. (2010a) is based on the assumption that the ratio of the variations of two quantities, e.g., CO₂ and relative humidity, is equal to the ratio of their vertical fluxes:

$$\frac{\partial \langle x_c \rangle}{\partial \langle RH \rangle} = \frac{\langle x'_c w' \rangle}{\langle RH' w' \rangle} \quad (4)$$

Prytherch et al. (2010a) derived Eq. (4) from the Monin–Obukhov similarity theory, assuming that the scalar profiles of the two non-dimensionalised quantities are equal.

The correction algorithm can be summarised as follows: first, the variations of x_c that are dependent on RH are removed from the measured signal x_{cm} with a 3rd order polynomial fit to the x_{cm} and RH time series:

$$x_c^0 = x_{cm} - \sum_{j=1:3} a_j (RH)^j \quad (5)$$

where a_j are the polynomial coefficients determined by the fit. A first-step CO₂ flux $F_c^{(0)}$ is calculated from the detrended signal $x_c^{(0)}$, and then used with Eq. (4) to get a first approximation of $\frac{\partial \langle x_c \rangle}{\partial \langle RH \rangle}$. The CO₂ mixing ratio is then adjusted using this quantity:

$$x_c^{(new)} = x_c^{(0)} + 0.5 \cdot (RH)' \cdot \frac{F_c^{(0)}}{\langle x'_c w' \rangle} \frac{\partial \langle x_c \rangle}{\partial \langle RH \rangle} \quad (6)$$

28290

Title Page

Abstract

Introduction

Conclusions

References

Tables

Figures

◀

▶

◀

▶

Back

Close

Full Screen / Esc

Printer-friendly Version

Interactive Discussion



Analysis of the PKT correction

S. Landwehr et al.

Title Page

Abstract

Introduction

Conclusions

References

Tables

Figures

◀

▶

◀

▶

Back

Close

Full Screen / Esc

Printer-friendly Version

Interactive Discussion



Here, the relative humidity flux $\langle RH' w' \rangle$ was substituted with $\langle x'_v w' \rangle \left(\frac{\partial \langle x_v \rangle}{\partial \langle RH \rangle} \right)^{-1}$, similar to Eq. (4). The adjusted time series $x_c^{(new)}$ is now used to calculate an approximation of the CO_2 flux via Eq. (4), and produce a new correction term for Eq. (6). Equations (4) and (6) are then looped until the CO_2 flux estimate converges to a flux value F_c^{PKT} (this loop typically converges within less than 10 steps). Equations (4–6) are taken from the Matlab code in the supplementary material of Prytherch et al. (2010a).

We found that the loop can be replaced by one simple equation:

$$F_c^{PKT} = F_c^{(0)} \cdot \beta \quad (7)$$

where $\beta = \left(1 - 0.5 \frac{\langle RH' w' \rangle}{\langle x'_v w' \rangle} \frac{\partial \langle x_v \rangle}{\partial \langle RH \rangle} \right)^{-1}$. From Eq. (4) it follows that $\beta \approx 2$.

In order to show this, we re-write Eq. (6) by replacing the adjusted mixing ratio $x_c^{(new)}$ with $x_c^{(j)}$ and $F_c^{(0)}$ with the flux from the previous iteration step $F_c^{(j-1)}$:

$$x_c^{(j)} = x_c^{(0)} + 0.5 \cdot \langle RH' \rangle \cdot \frac{F_c^{(j-1)}}{\langle x'_v w' \rangle} \frac{\partial \langle x_v \rangle}{\partial \langle RH \rangle} \quad (8)$$

Equation (8) is iterated within the PKT loop. The new flux estimate of iteration j (i.e. $F_c^{(j)}$) is computed from $x_c^{(j)}$ as follows:

$$F_c^{(j)} = F_c^{(0)} + 0.5 \cdot \langle RH' w' \rangle \cdot \frac{F_c^{(j-1)}}{\langle x'_v w' \rangle} \frac{\partial \langle x_v \rangle}{\partial \langle RH \rangle} \quad (9)$$

and is used to compute $x_c^{(j+1)}$ via Eq. (8). However, if Eq. (9) is inserted into the convergence criterion ($F_c^{(j)} - F_c^{(j-1)} \rightarrow 0$) and solved for $F_c^{(j-1)}$, we find that the loop will terminate at F_c^{PKT} given by Eq. (7). The results of the loop agree with Eq. (7) within the tolerance $|F_c^{(j)} - F_c^{(j-1)}| \leq 0.04 \text{ mol m}^{-2} \text{ yr}^{-1}$, which is used by Prytherch et al. (2010a) to

determine that the loop has converged. This can be seen in Fig. 3 (bottom), where the results of Eq. (7) are overlaid with F_c^{PKT} .

Prytherch et al. (2010a) validated the PKT method by applying it to the sensible heat flux as calculated from the measured speed of sound temperature (T_s). It has to be noted that the relative bias in the sensible heat caused by the humidity fluctuations is small (typically $\leq 10\%$). We followed this analysis and show our results in Fig. 8, which can be directly compared to Fig. 2 in (Prytherch et al., 2010a). The average of the flux, calculated from the detrended sonic temperature, yields approximately one half of the flux signal. The PKT flux, which is equal to the product of the detrended flux and β , correlates with the standard EC sensible heat flux. The scatter in the PKT-corrected fluxes is mostly derived from the scatter in $F_{T_s}^0$.

5 Discussion

The good agreement between the dried and un-dried CP systems for low latent heat fluxes (cp. Sect. 3.1) supports the findings of Miller et al. (2010) that application of a diffusion dryer does not alter the CO_2 flux signal, but avoids contamination of the sensor optics and significantly reduces the magnitude of the necessary air density correction.

The magnitude and scatter of the bias in the CO_2 flux results from the un-dried CP systems increased with the latent heat flux. These results are similar to results reported for OP IRGAs (LICOR-7500) (e.g Kondo and Osamu, 2007; Lauvset et al., 2011; Prytherch et al., 2010b), which showed an overestimation of the CO_2 compared to common bulk formulae. In this study, on the other hand, the bias reduced the CO_2 flux on average. Kondo and Tsukamoto (2012) simultaneously deployed OP (LICOR-7500) and CP (LICOR-7000) sensors to measure CO_2 fluxes in conditions with low air-sea CO_2 gradient ($12 \mu\text{atm} < \Delta p\text{CO}_2 < 42 \mu\text{atm}$) and large latent heat fluxes ($70 \text{ W m}^{-2} \leq \text{HI} \leq 140 \text{ W m}^{-2}$). The EC CO_2 flux estimates from both OP and CP IRGAs were an order of magnitude higher than expected using the Wanninkhof (1992)

Analysis of the PKT correction

S. Landwehr et al.

Title Page

Abstract

Introduction

Conclusions

References

Tables

Figures

◀

▶

◀

▶

Back

Close

Full Screen / Esc

Printer-friendly Version

Interactive Discussion



parametrisation and diverged increasingly for higher latent heat fluxes. We, therefore, assume that the bias observed in the fluxes from the un-dried CP has the same origin as the biases observed in the OP measurements cited above. Our measurements also indicate that the bias is different for each individual IRGA unit.

Equation (7) explains why the PKT correction produces unsatisfactory flux results: the PKT-corrected flux is simply a product of the flux signal, which was calculated from the CO₂ mixing ratios after detrending against the relative humidity, and the term $\beta \approx 2$ that depends solely on water vapour and relative humidity fluctuations. The ratio of the detrended fluxes of the two IRGA_{wet} analysers to the CO₂ flux measured by the IRGA_{dryB} and the factor β are plotted in Fig. 9 as a function of the latent heat flux. The parameter β shows a large scatter for low HI but converges to 2 for HI > 50 Wm⁻². The ratio of the detrended fluxes to the fluxes measured by the IRGA_{dry} ($(F_c^0) \cdot (F_c)^{-1}$) is on average close to 1 when latent heat flux is small, but exhibits large scatter. For HI > 50 Wm⁻² the value of F_c^0 becomes much smaller than F_c ; this leads to the observed underestimation by the PKT-corrected fluxes.

The PKT correction appears to correct the latent heat flux bias in the sonic sensible heat flux, because the flux calculated from the detrended sonic temperature yields on average approximately one half of the flux signal and is then multiplied with $\beta \approx 2$. However, this does not prove that the PKT correction can successfully remove the bias in the measured CO₂ fluxes.

6 Conclusions

Measurements of the air–sea CO₂ flux over the open ocean were conducted with four IRGAs, two of which had the water vapour fluctuations removed with a membrane dryer (Miller et al., 2010). The flux results from the dried and un-dried sensors agreed with each other only during periods of very low latent heat flux. With increasing latent heat flux, the CO₂ flux measurements from the un-dried sensors showed large scatter. This is similar to earlier studies Kondo and Osamu (2007); Lauvset et al. (2011); Prytherch

Analysis of the PKT correction

S. Landwehr et al.

Title Page

Abstract

Introduction

Conclusions

References

Tables

Figures

◀

▶

◀

▶

Back

Close

Full Screen / Esc

Printer-friendly Version

Interactive Discussion



et al. (2010b). However, in this study the bias flux was in average positive leading to a net reduction of the downward CO₂ flux.

The PKT correction was applied to the IRGA_{wet} measurement, and did reduce the range of the observed scatter from 1000 % to 100 % of the flux signal. The resultant PKT-corrected fluxes did however show only a weak correlation with the flux measurements from the IRGA_{dry}.

A detailed analysis of the PKT algorithm was performed, which revealed that the loop in the PKT correction can be replaced by a single equation that leads to the same results. Thus the PKT-corrected flux was found to be a product of the de-trended CO₂ flux and a factor that solely depends on the latent heat flux and relative humidity.

Therefore, the PKT method cannot be used to retrieve the CO₂ from the measured signal, since most CO₂ flux information is removed, along with the bias, by detrending. Conclusions made based on PKT-corrected CO₂ flux measurements should be treated with care.

Acknowledgements. This research was funded by Science Foundation Ireland as part of the US-Ireland R&D Partnership Programme under Grant Number 08/US/I1455 and US National Science Foundation Award 0851407, and by NIWA under Atmosphere Research Programme 2. Additional funding was provided by a SFI Short-term Travel Fellowship under Grant 09/US/I1758-STTF-11, and the EU FP7 project CARBOCHANGE under grant agreement no. 264879. We thank the captain and crew of the R/V *Tangaroa* who supported the measurements. Also thanks to Kim Currie who provided the $\Delta p\text{CO}_2$ data.

References

Bell, T. G., De Bruyn, W., Miller, S. D., Ward, B., Christensen, K., and Saltzman, E. S.: Air/sea DMS gas transfer in the North Atlantic: evidence for limited interfacial gas exchange at high wind speed, *Atmos. Chem. Phys. Discuss.*, 13, 13285–13322, doi:10.5194/acpd-13-13285-2013, 2013. 28286

Analysis of the PKT correction

S. Landwehr et al.

Title Page

Abstract

Introduction

Conclusions

References

Tables

Figures

◀

▶

◀

▶

Back

Close

Full Screen / Esc

Printer-friendly Version

Interactive Discussion



Analysis of the PKT correction

S. Landwehr et al.

Title Page

Abstract

Introduction

Conclusions

References

Tables

Figures

◀

▶

◀

▶

Back

Close

Full Screen / Esc

Printer-friendly Version

Interactive Discussion



Burns, S. P., Horst, T. W., Jacobsen, L., Blanken, P. D., and Monson, R. K.: Using sonic anemometer temperature to measure sensible heat flux in strong winds, *Atmos. Meas. Tech.*, 5, 2095–2111, doi:10.5194/amt-5-2095-2012, 2012. 28286

Edson, J. B., Hinton, A. A., Prada, K. E., Hare, J. E., and Fairall, C. W.: Direct covariance flux estimates from mobile platforms at sea, *J. Atmos. Ocean. Tech.*, 15, 547–562, 1998. 28282

Edson, J. B., Fairall, C. W., Bariteau, L., Zappa, C. J., Cifuentes-Lorenzen, A., McGillis, W. R., Pezoa, S., Hare, J. E., and Helmig, D.: Direct covariance measurement of CO₂ gas transfer velocity during the 2008 Southern Ocean Gas Exchange Experiment: wind speed dependency, *J. Geophys. Res.-Oceans*, 116, C00F10, doi:10.1029/2011JC007022, 2011. 28283, 28284, 28298

Ho, D., Law, C., Smith, M., Schlosser, P., Harvey, M., and Hill, P.: Measurements of air–sea gas exchange at high wind speeds in the Southern Ocean: implications for global parameterizations, *Geophys. Res. Lett.*, 33, L16611, doi:10.1029/2006GL026817, 2006. 28281

Kaimal, J. C., Wyngaard, J. C., Izumi, Y., and Coté, O. R.: Spectral characteristics of surface-layer turbulence, *Q. J. Roy. Meteor. Soc.*, 98, 563–589, 1972. 28281

Kohsiek, W.: Water vapor cross-sensitivity of open path H₂O/CO₂ sensors, *J. Atmos. Ocean. Tech.*, 17, 299–311, 2000. 28283, 28298

Kondo, F. and Osamu, T.: Air–sea CO₂ flux by eddy covariance technique in the equatorial indian ocean, *J. Oceanogr.*, 63, 449–456, 2007. 28282, 28283, 28292, 28293, 28298

Kondo, F. and Tsukamoto, O.: Comparative CO₂ flux measurements by eddy covariance technique using open- and closed-path gas analysers over the Equatorial Pacific Ocean, *Tellus B*, 64, 17511, doi:10.3402/tellusb.v64i0.17511, 2012. 28292, 28298

Lauvset, S. K., McGillis, W. R., Bariteau, L., Fairall, C. W., Johannessen, T., Olsen, A., and Zappa, C. J.: Direct measurements of CO₂ flux in the Greenland Sea, *Geophys. Res. Lett.*, 38, L12603, doi:10.1029/2011GL047722, 2011. 28283, 28284, 28292, 28293, 28298

Leuning, R. and King, K. M.: Comparison of eddy-covariance measurements of CO₂ fluxes by open- and closed-path CO₂ analysers, *Bound.-Lay. Meteorol.*, 59, 297–311, 1992. 28283

McGillis, W., Edson, J., Hare, J., and Fairall, C. W.: Direct covariance air–sea CO₂ fluxes, *J. Geophys. Res.*, 106, 16729–16745, 2001. 28282, 28283, 28298

McMillen, R.: An eddy correlation technique with extended applicability to non-simple terrain, *Bound.-Lay. Meteorol.*, 43, 231–245, doi:10.1007/BF00128405, 1988. 28286

Analysis of the PKT correction

S. Landwehr et al.

Title Page

Abstract

Introduction

Conclusions

References

Tables

Figures

◀

▶

◀

▶

Back

Close

Full Screen / Esc

Printer-friendly Version

Interactive Discussion



- Miller, S., Hristov, T., Edson, J., and Friehe, C.: Platform motion effects on measurements of turbulence and air–sea exchange over the open ocean, *J. Atmos. Ocean. Tech.*, 25, 1683–1694, 2008. 28282, 28285, 28286
- 5 Miller, S. D., Marandino, C., and Saltzman, E. S.: Ship-based measurement of air–sea CO₂ exchange by eddy covariance, *J. Geophys. Res.*, 115, D02304, doi:10.1029/2009JD012193, 2010. 28280, 28282, 28283, 28285, 28286, 28292, 28293, 28298
- Nightingale, P. D., Malin, G., Law, C. S., Watson, A. J., Liss, P. S., Liddicoat, M. I., Boutin, J., and Upstill-Goddard, R. C.: In situ evaluation of air–sea gas exchange parameterizations using novel conservative and volatile tracers, *Global Biogeochem. Cy.*, 14, 373–387, 2000. 28281
- 10 O'Sullivan, N., Landwehr, S., and Ward, B.: Mapping flow distortion on oceanographic platforms using computational fluid dynamics, *Ocean Sci.*, 9, 855–866, doi:10.5194/os-9-855-2013, 2013. 28287
- Popinet, S., Smith, M., and Stevens, C.: Experimental and numerical study of the turbulence characteristics of airflow around a research vessel, *J. Atmos. Ocean. Tech.*, 21, 1575–1589, 15 2004. 28287, 28301
- Prytherch, J., Yelland, M. J., Pascal, R. W., Moat, B. I., Skjelvan, I., and Neill, C. C.: Direct measurements of the CO₂ flux over the ocean: development of a novel method, *Geophys. Res. Lett.*, 37, L03607, doi:10.1029/2009GL041482, 2010a. 28280, 28283, 28284, 28286, 28288, 28290, 28291, 28292, 28298, 28307
- 20 Prytherch, J., Yelland, M. J., Pascal, R. W., Moat, B. I., Skjelvan, I., and Srokosz, M. A.: Open ocean gas transfer velocity derived from long-term direct measurements of the CO₂ flux, *Geophys. Res. Lett.*, 37, L23607, doi:10.1029/2010GL045597, 2010b. 28282, 28284, 28292, 28293
- Rowe, M. D., Fairall, C. W., and Perlinger, J. A.: Chemical sensor resolution requirements for near-surface measurements of turbulent fluxes, *Atmos. Chem. Phys.*, 11, 5263–5275, doi:10.5194/acp-11-5263-2011, 2011. 28282, 28287
- 25 Takahashi, T., Sutherland, S. C., Sweeney, C., Poisson, A., Metz, N., Tilbrook, B., Bates, N., Wanninkhof, R., Feely, R. A., Sabine, C., Olafsson, J., and Nojiri, Y.: Global sea–air CO₂ flux based on climatological surface ocean pCO₂, and seasonal biological and temperature effects, *Deep-Sea Res. Pt. II*, 49, 1601–1622, doi:10.1016/S0967-0645(02)00003-6, 2002. 28281
- 30 Wanninkhof, R.: Relationship between wind speed and gas exchange, *J. Geophys. Res.*, 97, 7373–7382, 1992. 28281, 28288, 28292, 28302

- Ward, B., Wanninkhof, R., McGillis, W. R., Jessup, A. T., DeGrandpre, M. D., Hare, J. E., and Edson, J. B.: Biases in the air–sea flux of CO₂ resulting from ocean surface temperature gradients, *J. Geophys. Res.*, 109, C08S08, doi:10.1029/2003JC001800, 2004. 28281
- 5 Webb, E. K., Pearman, G. I., and Leuning, R.: Correction of flux measurements for density effects due to heat and water vapour transfer, *Q. J. Roy. Meteor. Soc.*, 106, 85–100, 1980. 28282
- Yelland, M., Pascal, R., Taylor, P., and Moat, B. I.: AutoFlux: an autonomous system for the direct measurement of the air–sea fluxes of CO₂, heat and momentum, *Journal of Operational Oceanography*, 2, 15–23, 2009. 28282

Analysis of the PKT correction

S. Landwehr et al.

Title Page

Abstract

Introduction

Conclusions

References

Tables

Figures

I◀

▶I

◀

▶

Back

Close

Full Screen / Esc

Printer-friendly Version

Interactive Discussion



Analysis of the PKT correction

S. Landwehr et al.

Title Page

Abstract

Introduction

Conclusions

References

Tables

Figures

◀

▶

◀

▶

Back

Close

Full Screen / Esc

Printer-friendly Version

Interactive Discussion



Table 1. List articles that are relevant for the bias in NDIR CO₂ measurements that is related to relative humidity.

Publication	Configuration	Notes
Kohsiek (2000)	two custom-made NDIR sensors	Laboratory test show dependency of the CO ₂ on RH for RH ≥ 50%. Suggest water-films on the sensor optics as cause
McGillis et al. (2001)	LI-6262 closed-path with in-line particle filter	first air–sea EC CO ₂ fluxes consistent with bulk formulas
Kondo and Osamu (2007)	LI-7500 open-path	measured CO ₂ fluxes order of magnitude higher than bulk formula
Miller et al. (2010)	LI-7500 converted to closed-path, dried air-stream	reduced Webb correction CO ₂ fluxes consistent with bulk formula
Prytherch et al. (2010a)	LI-7500 open-path + PKT	suggest water films caused by salt particles as cause; order of magnitude correction
Lauvset et al. (2011)	LI-7500 open-path + PKT	order of magnitude correction
Edson et al. (2011)	LI-7500 shrouded + PKT and spectral method	small particles on sensor lenses; order of magnitude correction
Kondo and Tsukamoto (2012)	LI-7500 open-path and LI-7000 closed path	measured CO ₂ fluxes from both sensors order of magnitude higher than bulk formula
This study	LI-7500 Miller et al. (2010) compared to LI-7200 closed path + PKT	dry CO ₂ fluxes consistent with bulk formula; un-dried CO ₂ fluxes biased low; disproves PKT correction

Analysis of the PKT correction

S. Landwehr et al.

Table 2. Average CO₂ fluxes in [mol m⁻² yr⁻¹] for the complete experiment, and for subsets (Subset 1 [$-7 \text{ W m}^{-2} \leq \text{HI} \leq +7 \text{ W m}^{-2}$]; Subset 2 [$-35 \text{ W m}^{-2} \leq \text{HI} \leq -7 \text{ W m}^{-2}$]; Subset 3 [$+7 \text{ W m}^{-2} \leq \text{HI} \leq 340 \text{ W m}^{-2}$]) based on the latent heat flux measured by the IRGA_{wet}. To make the values comparable, only intervals with results from the PKT loop are used for the calculating the mean flux values.

Interval	all	Subset 1	Subset 2	Subset 3
# intervals	191	31	25	135
F_{cm} dryA	-6.69	-5.65	-5.15	-7.21
F_{cm} dryB	-6.76	-5.63	-5.31	-7.29
F_{cm} wetA	+6.54	-6.00	-6.19	+11.78
F_{cm} wetB	-2.34	-5.13	-6.16	-0.99
F_{PKT} wetA	-1.92	-5.41	-8.88	+0.18
F_{PKT} wetB	-2.59	-6.00	-8.10	-0.79

[Title Page](#)
[Abstract](#)
[Introduction](#)
[Conclusions](#)
[References](#)
[Tables](#)
[Figures](#)
[◀](#)
[▶](#)
[◀](#)
[▶](#)
[Back](#)
[Close](#)
[Full Screen / Esc](#)
[Printer-friendly Version](#)
[Interactive Discussion](#)


Analysis of the PKT correction

S. Landwehr et al.

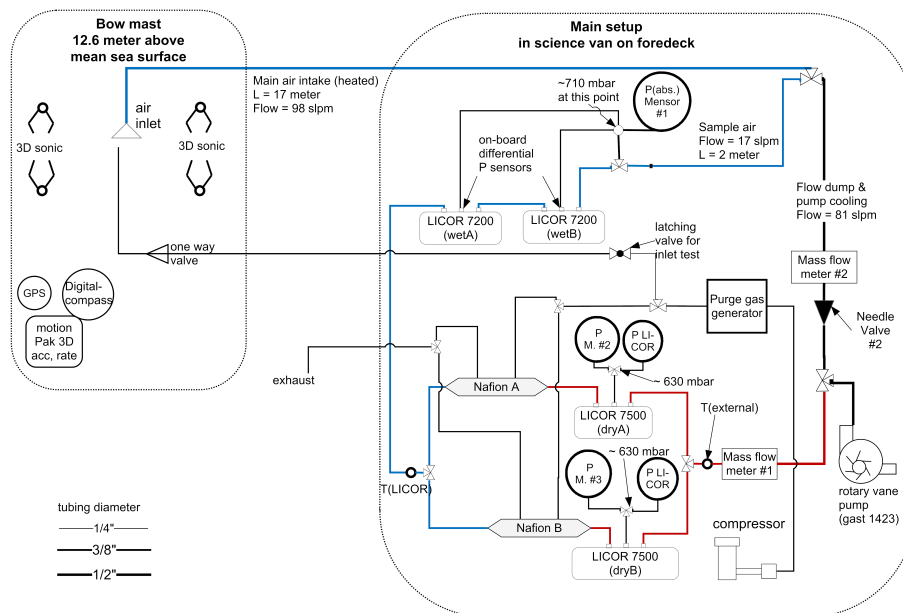


Fig. 1. Schematic of the Eddy Covariance setup for the SOAP experiment on the R/V *Tangorua*. The sample air line is colour-coded in blue and the colour is changed to red downstream of the membrane dryers to indicate that the air is dried at this point.

Title Page

Abstract

Introduction

Conclusions

References

Tables

Figures



Back

Close

Full Screen / Esc

Printer-friendly Version

Interactive Discussion



Analysis of the PKT correction

S. Landwehr et al.

Title Page

Abstract

Introduction

Conclusions

References

Tables

Figures

◀

▶

◀

▶

Back

Close

Full Screen / Esc

Printer-friendly Version

Interactive Discussion

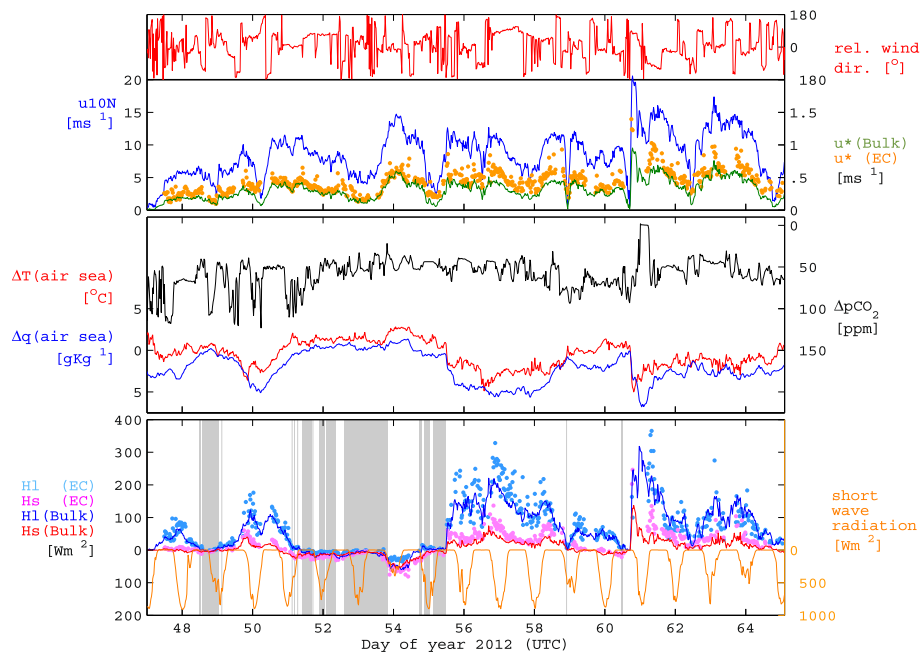


Fig. 2. Overview of conditions encountered during the SOAP experiment. The wind speed measurement was taken on the ship's main deck and is corrected for air-flow-distortion (Popinet et al., 2004) and normalised to standard conditions (10 m height and neutral stability). The bulk fluxes are calculated using this wind speed. All direct EC fluxes are measured at the bow mast using the Csats3 sonic anemometer and the IRGA in the science container on the fore-deck.

Analysis of the PKT correction

S. Landwehr et al.

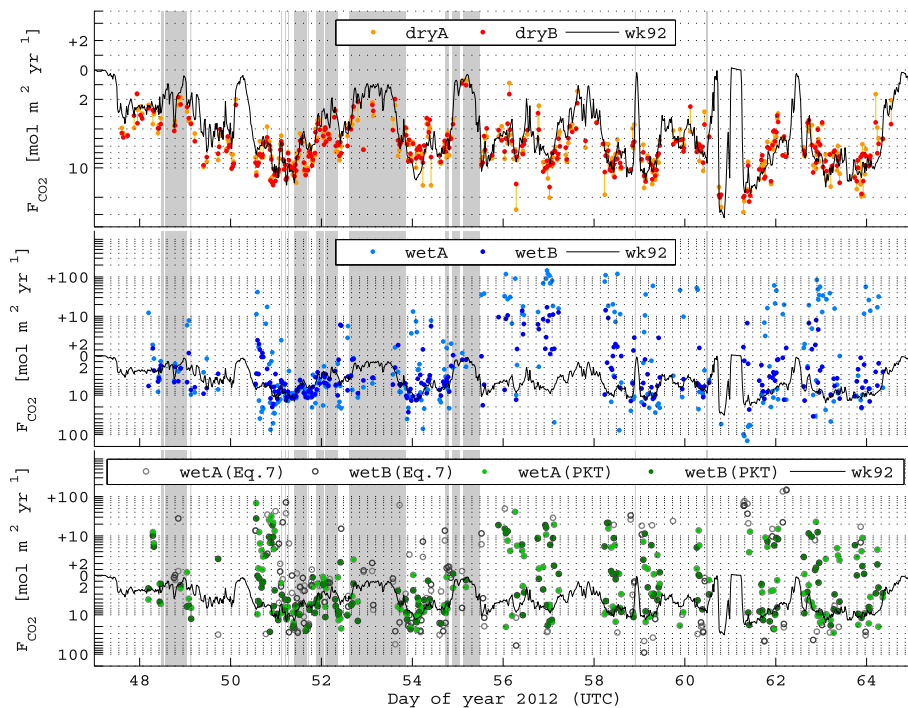


Fig. 3. Time series of the direct CO_2 fluxes and the parametrisation of Wanninkhof (1992), plotted on logarithmic scale with sign. Values between $\pm 2 \text{ mol m}^{-2} \text{ yr}^{-1}$ are plotted on linear scale. Shaded areas mark low latent heat fluxes ($\text{HI} \leq 7 \text{ W m}^{-2}$). Top: fluxes from the IRGA_{dry} parallel measurements are linked with vertical lines; middle: fluxes from IRGA_{wet} ; bottom: fluxes from IRGA_{wet} after the PKT correction has been applied to the CO_2 measurements and the results from Eq. (7), which are overlaid with the PKT results.

Title Page

Abstract

Introduction

Conclusions

References

Tables

Figures

◀

▶

◀

▶

Back

Close

Full Screen / Esc

Printer-friendly Version

Interactive Discussion



Analysis of the PKT
correction

S. Landwehr et al.

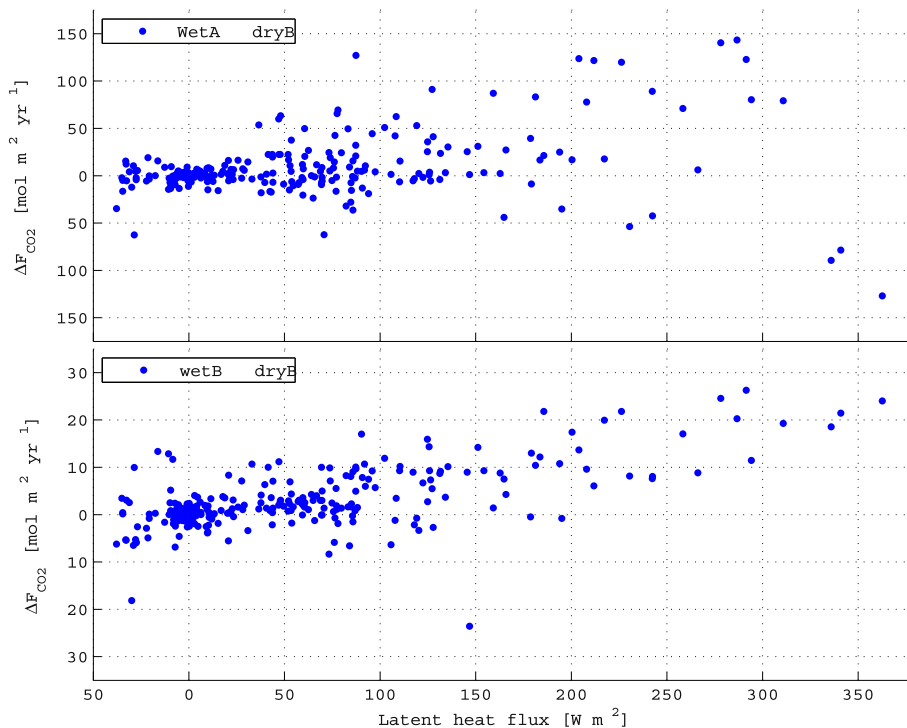


Fig. 4. Difference of the CO_2 flux calculated from the measured IRGA_{wet} signals x_{cm} to the flux from $\text{IRGA}_{\text{dryB}}$ as a function of the latent heat flux calculated from the IRGA_{wet} signals. Different scales are used for the two sub-plots.

Title Page

Abstract

Introduction

Conclusions

References

Tables

Figures

◀

▶

◀

▶

Back

Close

Full Screen / Esc

Printer-friendly Version

Interactive Discussion



Analysis of the PKT correction

S. Landwehr et al.

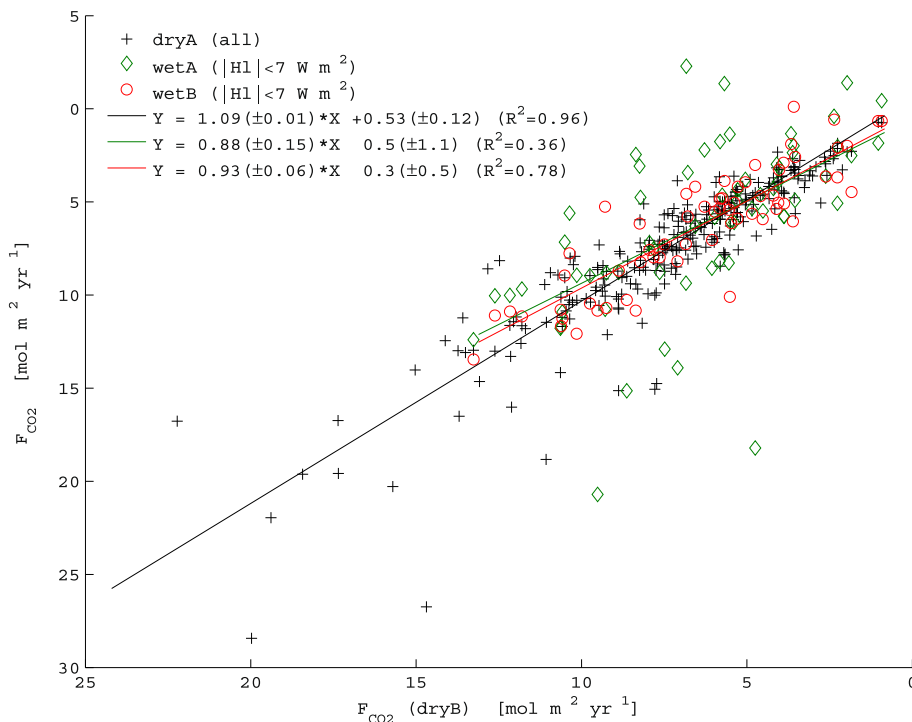


Fig. 5. Scatter plot of the CO_2 flux measurements (without PKT correction) from $\text{IRGA}_{\text{wetA}}$, $\text{IRGA}_{\text{wetB}}$ and $\text{IRGA}_{\text{dryA}}$ against those from $\text{IRGA}_{\text{dryB}}$. For IRGA_{wet} , only measurements with $HI \leq 7 \text{ W m}^{-2}$ are used. Linear fit coefficients with standard deviation and the R^2 value are shown in the legend.

Title Page

Abstract

Introduction

Conclusions

References

Tables

Figures

◀

▶

◀

▶

Back

Close

Full Screen / Esc

Printer-friendly Version

Interactive Discussion



Analysis of the PKT correction

S. Landwehr et al.

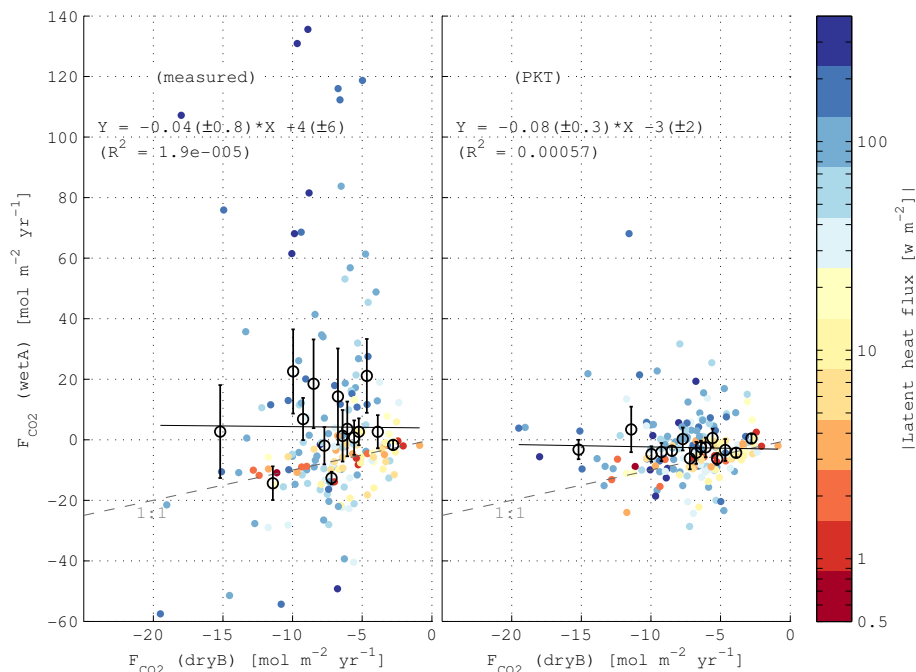
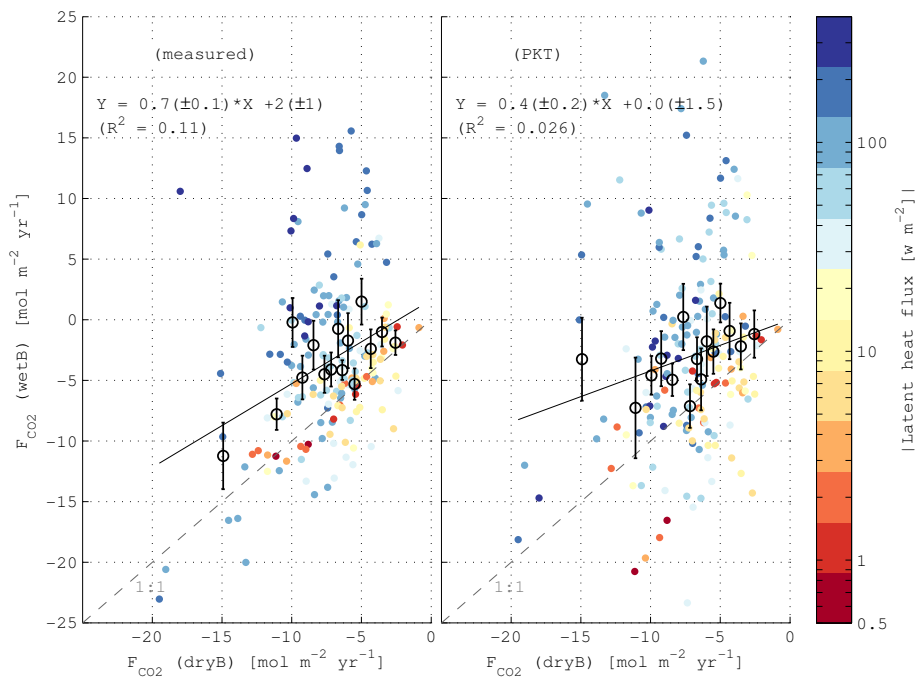


Fig. 6. Scatter plot of the CO_2 flux measurements from $\text{IRGA}_{\text{wetA}}$ against those from $\text{IRGA}_{\text{dryB}}$ before (left) and after the PKT correction was applied to the $\text{IRGA}_{\text{wetA}}$ measurements (right). Bin averages of 15 bins with an equal number of data points are shown as black circles, with error bars indicating the standard deviation from the bin average. A linear regression to the data is shown as solid black line and the 1 : 1 agreement is indicated with a grey dashed line. Only intervals for which the PKT correction provided a result were used for this plot.

Analysis of the PKT correction

S. Landwehr et al.

Fig. 7. Same as Fig. 6, but for IRGA_{WetB}.

Title Page

Abstract

Introduction

Conclusions

References

Tables

Figures

◀

▶

◀

▶

Back

Close

Full Screen / Esc

Printer-friendly Version

Interactive Discussion

Analysis of the PKT correction

S. Landwehr et al.

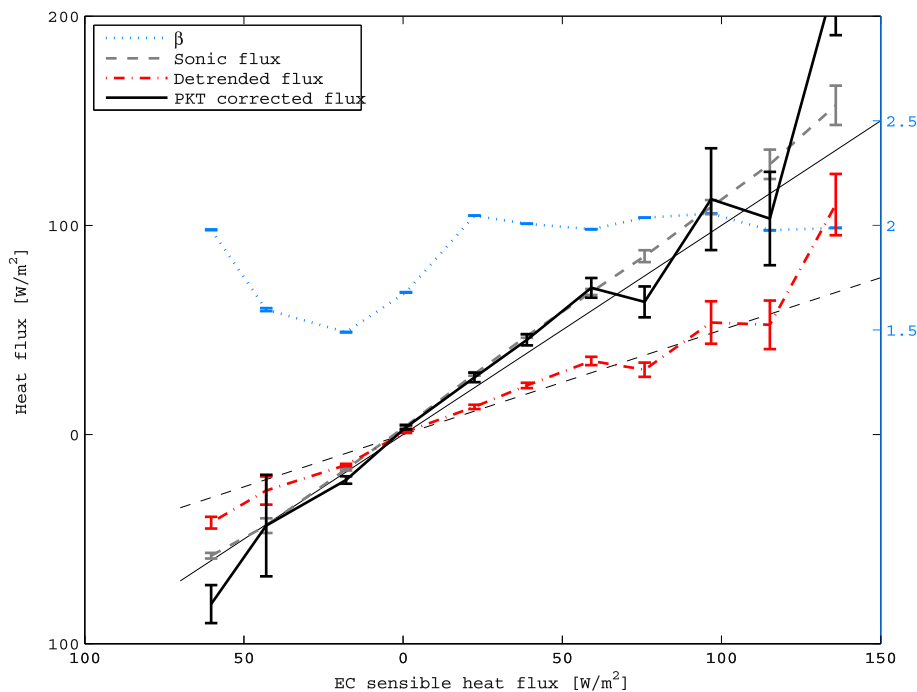


Fig. 8. Bin-averaged heat fluxes plotted against the standard EC sensible heat flux results (to be compared with Fig. 2 in Prytherch et al., 2010a): “sonic flux” calculated from T_s (light grey - -); flux after detrending against humidity (red - · -); “PKT-corrected” flux (black -). The bin averages and standard deviations of β from Eq. (7) are plotted on the right axis. Error bars show standard deviation from the mean. The thin black line shows the 1 : 1 agreement and the dashed line the 1 : 2 agreement, respectively.

Title Page

Abstract

Introduction

Conclusions

References

Tables

Figures

◀

▶

◀

▶

Back

Close

Full Screen / Esc

Printer-friendly Version

Interactive Discussion



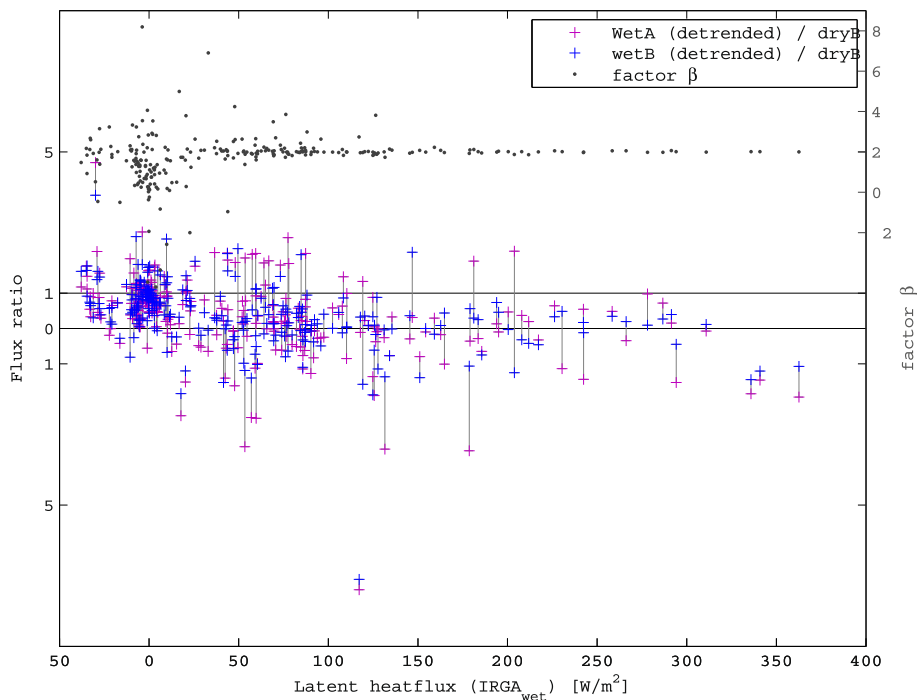


Fig. 9. Ratio of the detrended CO₂ fluxes F_c^0 from IRGA_{wet} as used for the PKT correction to the average CO₂ flux calculated from the two IRGA_{dry} (purple +, blue +). Two values of the

same sample interval are connected with a grey line; the factor $\beta = \left(1 - 0.5 \frac{\langle RH' w' \rangle}{\langle x' w' \rangle} \frac{\partial \langle x \rangle}{\partial \langle RH \rangle}\right)^{-1}$ as in Eq. (7), calculated from the latent heat flux and relative humidity, as measured by IRGA_{wet}, (grey •). The PKT-corrected fluxes are the product of F_c^0 and β . The black lines indicate the ratios zero and one.

[Title Page](#)
[Abstract](#)
[Introduction](#)
[Conclusions](#)
[References](#)
[Tables](#)
[Figures](#)
[◀](#)
[▶](#)
[◀](#)
[▶](#)
[Back](#)
[Close](#)
[Full Screen / Esc](#)
[Printer-friendly Version](#)
[Interactive Discussion](#)
